Article:
González-Santana, A., Estévez-Herrera, J., Seward, E.P. orcid.org/0000-0001-5311-1343 et al. (2 more authors) (2021) Glucagon-like peptide-1 receptor controls exocytosis in chromaffin cells by increasing full-fusion events. Cell Reports, 36 (8). 109609. ISSN 2639-1856

https://doi.org/10.1016/j.celrep.2021.109609

Cell Reports

Article

Glucagon-like peptide-1 receptor controls exocytosis in chromaffin cells by increasing full-fusion events

Graphical abstract

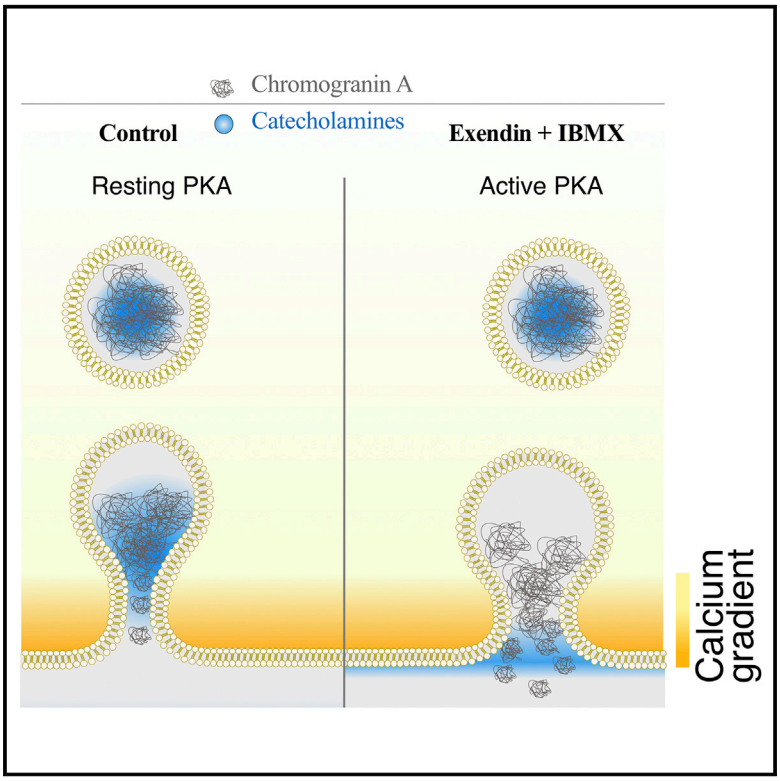

Highlights

- Activation of a G-protein-coupled receptor (GLP-1R) modulates exocytosis
- GLP-1R controls the amount of transmitter released *per quanta*
- GLP-1R shifts the mode of exocytosis from partial to full fusion

Authors

Ayoze González-Santana, Judith Estévez-Herrera, Elizabeth P. Seward, Ricardo Borges, José David Machado

Correspondence

david.machado@ull.edu.es

In brief

GLP-1R regulates exocytosis in adrenal chromaffin cells. González-Santana et al. demonstrate that activation of this G-protein-coupled receptor increases cargo release from secretory vesicles by a shift from partial- to full-fusion exocytotic mode.

González-Santana et al., 2021, Cell Reports *36*, 109609
August 24, 2021
https://doi.org/10.1016/j.celrep.2021.109609

CellPress

Cell Reports

CellPress
OPEN ACCESS

Article

Glucagon-like peptide-1 receptor controls exocytosis in chromaffin cells by increasing full-fusion events

Ayoze González-Santana,[1] Judith Estévez-Herrera,[1] Elizabeth P. Seward,[2] Ricardo Borges,[1] and José David Machado[1,3,*]
[1]Unidad de Farmacología, Facultad de Medicina, Universidad de La Laguna, 38200 La Laguna, Tenerife, Spain
[2]Department of Biomedical Science, Firth Court, University of Sheffield, Western Bank, Sheffield S10 2TN, UK
[3]Lead contact
*Correspondence: david.machado@ull.edu.es
https://doi.org/10.1016/j.celrep.2021.109609

SUMMARY

Agonists for glucagon-like-peptide-1 receptor (GLP-1R) are currently used for the treatment of type 2 diabetes and obesity. Their benefits have been centered on pancreas and hypothalamus, but their roles in other organ systems are not well understood. We studied the action of GLP-1R on secretions of adrenal medulla. Exendin-4, a synthetic analog of GLP-1, increases the synthesis and the release of catecholamines (CAs) by increasing cyclic AMP (cAMP) production, without apparent participation of cAMP-regulated guanine nucleotide exchange factor (Epac). Exendin-4, when incubated for 24 h, increases CA synthesis by promoting the activation of tyrosine hydroxylase. Short incubation (20 min) increases the quantum size of exocytotic events by switching exocytosis from partial to full fusion. Our results give a strong support to the role of GLP-1 in the fine control of exocytosis.

INTRODUCTION

Adrenal catecholamines (CAs) actively participate in the adaptive mechanisms used to restore body homeostasis in the body, especially in response to stress conditions such as hypoglycemia, cold, hypotension or fear (Goldstein, 2010). Like all neuroendocrine cells, chromaffin cells exert their control of body functions through the secretion of stored transmitters into the blood stream using regulated exocytosis. Stored within their large dense core vesicles (also called chromaffin granules) is a cocktail of small molecules, such as adrenaline, noradrenaline, and ATP, as well as bioactive peptides, granins, and enkephalins. Because of the neural origin of chromaffin cells, the nature of their secretory products, and the basic mechanisms of regulating exocytosis, chromaffin cells have been a widely used model for the study of the molecules that control vesicle fusion (Jahn et al., 2003; Neher, 2018; Neher and Marty, 1982; Wightman et al., 1991). As the amount of CA stored in the adrenal medulla is enough to kill an individual, the processes controlling their secretion must by tightly regulated. Classically, the main mechanism considered for this regulation is by receptor-operated mechanisms leading to variation in the number of secretory vesicles that undergo exocytosis, either through modulation of the number of ''readily releasable'' vesicles available to respond to a stimulus and/or the calcium signals that regulate vesicle priming and fusion (Bauer et al., 2007; Gillis et al., 1996; Neher and Sakaba, 2008; Powell et al., 2000; Yim et al., 2018). However, because the amount of secretory products released by each quantal fusion (partial versus full fusion) and its kinetics are subject to regulation (Álvarez de Toledo et al., 2018; Shin et al., 2018), this raises the possibility that even this late stage of exocytosis may be modulated by receptors.

The insulinotropic hormone glucagon-like peptide-1 (7-36)-amide (GLP-1) has potent effects on glucose-dependent insulin secretion, insulin gene expression, and pancreatic islet cell formation (Baggio and Drucker, 2007; Doyle and Egan, 2007; Müller et al., 2019). Both peptide agonists of the GLP-1 receptor (GLP-1R) (e.g., exendin-4 [Ex-4]) and inhibitors of GLP-1 degradation (e.g., DPP-4) are used clinically for this purpose in diabetes treatment. Since adrenaline plays a key role in counter-regulation and recovery from hypoglycemia (Verberne et al., 2016; Vollmer et al., 1997), it seems plausible that GLP-1R in chromaffin cells could be involved in the fine regulation of glycaemia, especially under stressed conditions.

In this study, we have addressed the question of whether the incretin receptor GLP-1R regulates adrenal chromaffin secretory responses by examining the effects on CA content, secretion, and kinetics of single exocytotic events.

RESULTS

The GLP-1 incretin receptor is expressed in chromaffin cells

The expression of GLP-1R mRNA in bovine chromaffin cells was verified by RT-PCR (Figure S1) and its localization determined by immunocytochemistry and confocal microscopy. Chromaffin cells were positively identified by labeling with antibodies against tyrosine hydroxylase (TH); over 95% of cells in our cultures were labeled as TH positive. In unpermeabilized, intact cells, GLP-1R immunoreactivity was restricted to the plasma membrane

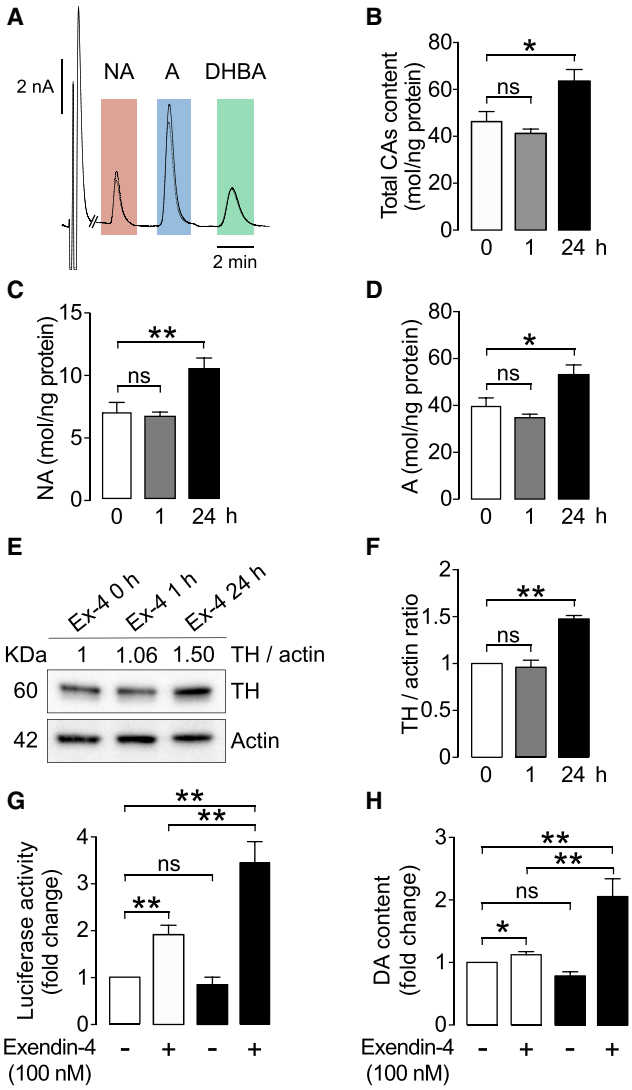

Figure 1. Ex-4 increases catecholamine (CA) biosynthesis and TH expression in chromaffin cells

(A) Superimposed chromatograms showing the noradrenaline (NA), adrenaline (A), and DHBA (internal standard) measured in untreated (dashed line) and cells treated for 24 h with Ex-4 (solid line). Amine content in lysates was analyzed by high-performance liquid chromatography (HPLC).

(B) Average total CA content in lysates from untreated cells and cells treated with Ex-4 for 1 or 24 h, as indicated.

(C and D) Average adrenaline and noradrenaline content in the same lysates described in (B).

(E) Representative western blot of TH expression carried out 0, 1 and 24 h after treatment with Ex-4. Equal amounts of protein (21 μg/lane). Actin was used as an internal loading control.

(F) Quantification of TH expression expressed as the TH/actin ratio from three or four experiments.

(G) Ex-4 increases transcription of the gene for TH and dopamine content. PC12 cells, transiently nucleofected with p5′TH-Luc (−272/+27) and EGFP (open bars) or GLP-1R-EGFP (filled bars), were treated for 12 h with Ex-4 (100 nM) and compared to untreated cells (control). Cell lysates were assayed for firefly luciferase activity and normalized to protein concentration as described in STAR Methods (n = 10 lysates of 1 × 10^6 cells per condition).

(H) In parallel experiments, total dopamine content in EGFP- and GLP-1R-EGFP-expressing cells was measured by HPLC (n = 7 lysates of 1 × 10^6 cells per condition).

Data shown (B)–(D) are the means ± SEM for n = 6 replicates of 1.5 × 10^6 cells per condition; *p < 0.05 (ANOVA; Dunnett's multiple comparisons test). Data presented in (G) and (H) are means ± SEM of two independent cell cultures; *p < 0.05 and **p < 0.01 (ANOVA; Dunnett's multiple comparisons test).

(Figure S2A), whereas in permeabilized cells, fluorescence was prominent in subcellular compartments exhibiting a punctuated distribution (Figure S2B). Similar results have been described where the receptor is mainly located in the plasma membrane and in intracellular compartments visualized a punctuated distribution that co-localizes with caveolin-1 (Jones et al., 2018; Syme et al., 2006; Thompson and Kanamarlapudi, 2015). Conversely, TH fluorescence appeared diffuse throughout the cell interior. Western blotting of enriched plasma membrane fractions isolated from PC12 shows two bands in the lane of GLP-1R (Figure S3). These have been described also in the Beta-TC-6 cell line and correspond to different forms of GLP-1R (canonical and glycosylated) (Zhou et al., 1999)."

Ex-4 increases expression of TH and CA synthesis in chromaffin cells

To test the effect of the activation of GLP-1R on CA synthesis, we incubated chromaffin cells with Ex-4 (100 nM; for 1 and 24 h). Ex-4 is a high-affinity, potent agonist at GLP-1R which is known to activate the full complexity of signaling observed with GLP-1 but, with the added benefit of being resistant to degradation (Fletcher et al., 2016). As shown in Figure 1, after 24-h exposure to Ex-4, the total CA content of chromaffin cells is significantly increased (Figures 1A and 2B). This increase occurred for both noradrenaline and adrenaline (Figures 1C and 1D). By comparison, treatment with Ex-4 for only 1 h did not increase total CA content, consistent with a slower, possibly transcription-dependent signaling event following GLP-1R, as has been reported in other cells expressing the receptor (Sonoda et al., 2008). Because TH catalyzes the rate-limiting step in CA biosynthesis and is known to be a highly regulated enzyme (Dickson and Briggs, 2013) whose transcription may be regulated by cAMP responsive element binding protein (CREB/ (Piech-Dumas and Tank, 1999), a downstream target of GLP-1R-mediated cyclic AMP (cAMP) signals, we tested whether the increase in CA after GLP-1R activation was due to an increase in the activity or amount of TH. Western blot analyses showed increased expression of TH only after 24-h treatment with Ex-4 (Figures 1E and 1F). Taken together, the results indicate that prolonged GLP-1R activation in chromaffin cells increases CA biosynthesis in both adrenergic and noradrenergic cells by increasing TH gene expression.

Ex-4 enhances TH gene expression in PC12

In β cells, GLP-1R cAMP signaling increases proinsulin gene transcription and subsequent insulin biosynthesis (Fletcher et al., 2016), and since the TH promoter also contains response elements to cAMP (Fader and Lewis, 1990), we measured the effect of Ex-4 on transcription of the TH gene with a luciferase reporter assay. PC12 cells were transfected with p5′TH-Luc (−272 / + 27) and GLP-1R-EGFP or EGFP and treated with

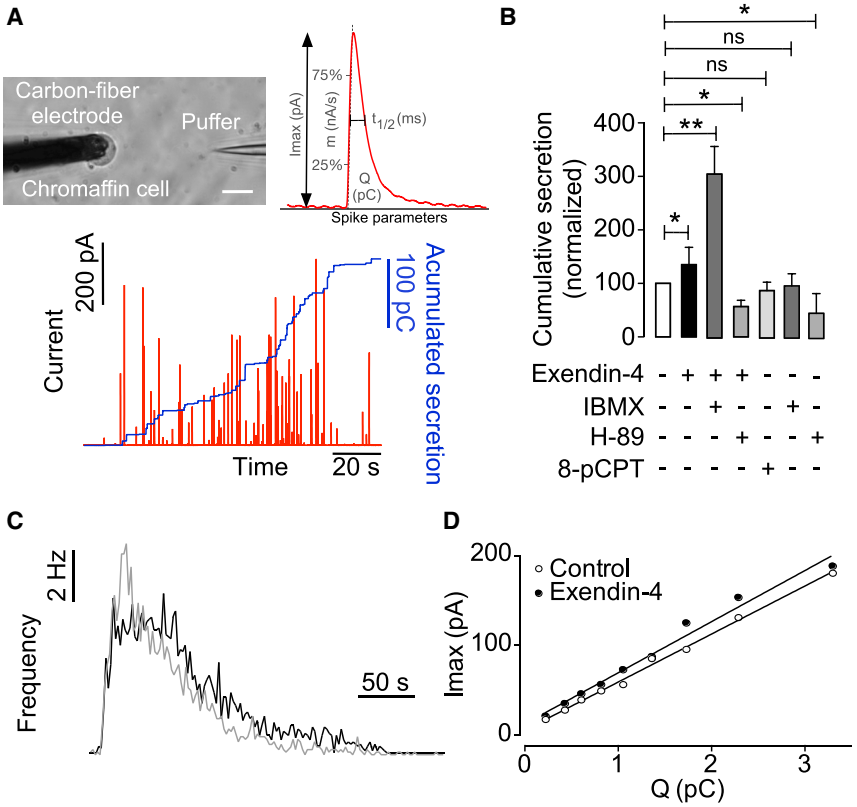

Figure 2. Ex-4 potentiates the secretion of CA

(A) Typical amperometric recording from a control cell showing a characteristic firing pattern of exocytosis after barium injection (red trace) and the cumulative secretion obtained by integrating the amperometric signal measured for 2 min, expressed as pico-Coulombs (pC) (superimposed blue trace). Inset: representative image showing the position of the carbon-fiber electrode on the top of a single chromaffin cell and the glass pipette used for secretagogue injection (puffer) to the right of the cell. Secretion was elicited by a 5-s pressure ejection of 5 mM Ba^{2+}. After stimulation, the micropipette was moved up 1 mm using a motorized micromanipulator to avoid any effects of unwanted leakage. Scale bar, 15 μm. Parameters obtained from each secretory spike: I_{max}, maximum oxidation current; $t_{1/2}$, spike width at the half-height; Q, net CA charge; m, ascending slope of the spike.

(B) Bars show cumulative secretion pooled from different cells obtained in the absence (n = 10) or presence of 100 nM Ex-4 (n = 12) and 500 μM IBMX (n = 10), 50 nM H-89 (n = 14), 100 μM 8-pCPT (n = 17), 500 μM IBMX (n = 13), or 50 nM H-89 (n = 7) as indicated (all drugs were incubated for 20 min before recording). Bars show normalized secretion obtained in the absence or presence of 100 nM Ex-4. Data are mean ± SEM; *p < 0.05 and**p < 0.01, Mann-Whitney U test with the Bonferroni correction. Data are from the same experiment summarized in Table 1.

(C) Spike frequency analysis of cells treated with Ex-4 (black trace) and untreated cells (gray trace) Mean ± SEM, 1.48 ± 0.3 versus 1.69 ± 0.3; p = 0.63, Student's t test.

(D) Spike amplitude (I_{max}) versus quantum size (Q) of secretory spikes from cells treated with Ex-4 and untreated cells (control) and linear fits (slopes: 54 ± 1 (control) versus 57 ± 3 (Ex-4); p = 0.3101.

100 nM Ex-4 for 12 h. As shown in Figure 1G, Ex-4 stimulated transcription ~2-fold in PC12 expressing endogenous levels of GLP-1R and ~3-fold when the receptor was overexpressed. No significant differences were observed between untreated cells regardless of receptor expression, confirming the effects of Ex-4 were a consequence of GLP-1R activation.

To ascertain whether the increased TH expression correlated with increased CA biosynthesis, we quantified the effects of Ex-4 on dopamine content in EGFP-transfected PC12 cells and cells overexpressing GLP-1R-EGFP. Consistent with the observations made in chromaffin cells, 12-h treatment of PC12 cells with Ex-4 increased dopamine (DA) biosynthesis (Figure 1H), in line with the increased expression of the TH gene.

Single-cell amperometry reveals an increase in the amount of CA released per vesicle in cells treated with Ex-4

Cells were stimulated by pressure application of 5 mM $BaCl_2$ for 5 s from a micropipette located ~40 μm from the cell (Figure 2A; Baraibar et al., 2018). To avoid bias, measurements were made on the same day using a calibrated carbon fiber electrode and alternating between control cells and those treated with 100 nM Ex-4 for 20 min. We used this period of time in order to discard the hypothesis that increases in Q size upon Ex-4-treated cells is caused by newly synthesized CA.

Ex-4 induced an increase of secretion (Figure 2B) caused mostly by enhance ~75% of the quantum CA release size (Q) of the vesicles (Table 1). Conversely, the frequency of secretory events, defined as the number of spikes per unit time, showed no significant difference following treatment with Ex-4 (mean ± SEM, 1.48 ± 0.3 [control] versus 1.69 ± 0.3 [Ex-4-treated cells]; p = 0.63, Student's t test) (Figure 2C). Therefore, the ~35% increase in total CA secretion recorded over 120 s after stimulation was caused through the increase in quantum size.

Analysis of stimulus evoked amperometric spikes showed further that acute exposure to Ex-4 significantly increases I_{max}, Q, and apparent foot duration (Table 1). As I_{max} and Q are tightly related parameters, we plotted I_{max} versus Q (Figure 2E) and observed, as expected, a linear relationship. The analysis of slopes shows a similar kinetics (slopes: 54 ± 1 [pA/pC; control] versus 57 ± 3 [(pA/pC; Ex-4]; p = 0.3101), indicating that CA secretion is similar in Ex-4-treated and untreated cells.

The increase in apparent foot duration observed when Ex-4 is applied is directly related with the increase in quantal size

These results again suggest that the increase in CA secreted following activation of GLP-1R is caused by more CA being released from each vesicle and not as a result of an increase in the number of exocytotic events per stimuli.

Table 1. Amperometric spike characteristics are altered in chromaffin cells treated with Ex-4

	I_{max} (pA)	Q (pC)	$t_{1/2}$ (ms)	m (pA/ms)	N (cells)	n (spikes)	Foot (ms)	n
Control	85.6 ± 11	1.2 ± 0.1	19.4 ± 2	18.8 ± 3	10	647	4.3 ± 0.2	628
Ex-4	126.4 ± 13*	2.1 ± 0.3*	15.1 ± 1	29.8 ± 3*	12	1166	4.9 ± 0.2**	1156
Change	+47.7%	+75%	−22.2%	+58.5%				

This is a representative experiment from two carried out on independent cell cultures; recordings were performed by alternating between cells treated with Ex-4 and control untreated cells. Data are expressed as means ± SEM in the units in parentheses. In all cases, *p < 0.05 (Mann-Whitney *U* test).

GLP-1R overexpression intensifies the effect of Ex-4

As a further verification to show that the effects of Ex-4 on increasing CAs secretion in chromaffin cells is mediated by the activation of GLP-1R, we next examined the impact of overexpressing the receptor on secretory responses. Bovine chromaffin cells were nucleofected with GLP-1R-EGFP plasmid. Cells with overexpressed receptor can be distinguished because of the fluorescence emitted by EGFP (Figure S4A). Using only the fluorescent cells, single cell amperometry was used to compare cells treated with 100 nM Ex-4 for 20 min with untreated cells.

Treatment with Ex-4 on cells overexpressing GLP-1R-EGFP resulted in 38% increase in quantum size (see Figure S4, table, Q), which is smaller than the increased quantum CA size observed in cells treated with Ex-4 where GLP-1R was not overexpressed (note the quantitative differences between controls intact cells with those transfected by nucleofection in Table 1 and the table in Figure S4).

In agreement with results obtained from untransfected cells, Ex-4 did not produce a significant increase in the frequency of secretory events recorded in response to stimulation in cells overexpressing the receptor (Figure S4C); however, the duration of stimuli-evoked increases in spike frequency was notably briefer in cells overexpressing the receptor compared with untransfected cells. Despite the lack of increases in the number of stimulus-evoked secretory events (Figure S4), and in agreement with results from untransfected cells, 20-min treatment with Ex-4 again increased total CA secretion by 70% (142 pC in control cells versus 243 pC in cells treated with Ex-4) (Figure S4B), consistent with an effect on quantum size.

Analysis of individual spike parameters in GLP-1R overexpressing cells, showed that Ex-4 resulted in increased I_{max} and Q, with a non-significant decrease in $t_{1/2}$ (see Figure S4, table). Examining the relationship between I_{max} and Q further, showed a change in slope (83 ± 3 (pA/pC; control) versus 101 ± 2 (pA/pC; Ex-4); p = 0.002) indicating that Ex-4 increased the speed of CA secretion from single vesicles (Figure S4D).

The increase in CA secretion is due to activation of the intracellular pathway mediated by PKA

Canonical signaling by GLP-1R is predominantly mediated by activation of G proteins and increases in cAMP; in β cells, where the underlying signals generated by GLP-1 and Ex-4 have been investigated, downstream activation of protein kinase A (PKA) and cAMP-regulated guanine nucleotide exchange factor (Epac) accounts for enhanced insulin synthesis and secretion (Fletcher et al., 2016). To elucidate the intracellular pathways that give rise to increased CA secretion from chromaffin cells, we used single-cell amperometry to determine how CA secretion was modified in response to drugs that interfere with cAMP signaling. Incubation with the nonspecific phosphodiesterase inhibitor 3-isobutyl-1-methyl-xanthine (IBMX) to prevent cAMP degradation and slightly increase basal cellular cAMP levels in the absence of agonist does not induce an increase in CA secretion in chromaffin cells (Machado et al., 2001); however, when added together with 100 nM Ex-4 for 20 min, an increase CA secretion was observed, which was significantly larger than that observed with Ex-4 alone (Figure 2B). Moreover, this was accompanied by increases in I_{max} and Q, consistent with an effect on quantum size (Table 2). Cell treatment with 50 nM H-89, an inhibitor of the catalytic activity of PKA, co-incubated for 20 min with 100 nM Ex-4 by contrast, ablated the increase in total CA secretion caused by Ex-4 (Figure 2C) and decreased the quantum CA size by ~36% (Table 2). Finally, incubation with 100 μM 8-pCPT (8-(4-chlorophenylthio) −2′-O-methyladenosine-3′, 5′-cyclic monophosphate acetyl methyl ester) to directly activate the Epac pathway was found to have no significant potentiating effect on CA secretion from chromaffin cells (Figure 2B; Table 2). When Ex-4 is added with 8-pCPT, no significant increase in the quantal size was measured.

These data indicate that GLP-1R activation increases CA secretion from chromaffin cells through the activation of a second messenger pathway mediated by cAMP and PKA, without the apparent involvement of the Epac pathway.

Ex-4 does not affect exocytosis or Ca^{2+} currents measured by membrane capacitance

Although our amperometry experiments indicated that Ex-4 did not increase the number of vesicles undergoing exocytosis in response to a stimulus, we wanted to test this independently by directly measuring vesicle fusion using membrane capacitance (Cm) measurements. Cells were voltage clamped in the whole-cell patch-clamp configuration, and exocytosis was evoked with a train of 6 × 10 ms depolarizations followed by 4 × 100 ms depolarizations to distinguish between the immediately releasable vesicle pool and the readily and slowly releasable pools (Voets, 2000). The activation of GLP-1R with 100 nM Ex-4 did not significantly increase evoked exocytosis measured in response to either the short or long depolarizations (Figure S4). Moreover, the calcium currents measured using the same protocol were also unaffected by Ex-4 (Figure S4). A lack of effect of Ex-4 on calcium signaling was also confirmed using calcium imaging (Figure S5), which shows that after nicotinic stimulation, there is no significant contribution from intracellular calcium stores (Mollard et al., 1995). We therefore concluded from these experiments that the number of vesicles undergoing fusion with the plasma membrane is not significantly higher in cells

Table 2. Amperometry spike characteristics obtained in chromaffin cells treated with IBMX, H-89, and 8-pCPT in the presence or absence of Ex-4

Experiment	I_{max} (pA)	Q (pC)	$t_{1/2}$ (ms)	m (pA/ms)	n (cells)
Control	30.5 ± 3	1.3 ± 0.1	36.9 ± 3	6.2 ± 2	15
IBMX	22.0 ± 3*	1.3 ± 0.2	46.4 ± 2*	3.7 ± 1*	13
Change	−28.0%	+1%	−25.7%	41.2%	
Control	58.9 ± 4	1.4 ± 0.1	19.5 ± 2	8.5 ± 1	9
IBMX + Ex-4	110.7 ± 13**	2.2 ± 0.3*	16.4 ± 1	18.2 ± 2**	10
Change	+87.9%	+57.1%	−15.9%	+114.1%	
Control	26.7 ± 2.5	0.9 ± 0.1	32.2 ± 1	3.0 ± 1	9
H-89	32.3 ± 6.6*	0.7 ± 0.1*	26.1 ± 1*	4.4 ± 1*	7
Change	+21.0%	−22.2%	−18.9%	46.6%	
Control	67.9 ± 10	1.4 ± 0.2	17.5 ± 1	8.1 ± 1	13
H-89 + Ex-4	52.5 ± 6	0.9 ± 0.1*	14.1 ± 1*	6.9 ± 1	14
Change	−22.7%	−35.7%	−19.4%	−14.8%	
Control	58.1 ± 1	1.0 ± 0.1	13.6 ± 1	12.3 ± 2	13
8pCPT	63.4 ± 6	1.1 ± 0.1	14.7 ± 1	14.7 ± 2	17
Change	+10.4%	+10.0%	+8.1%	+14.6%	
Ex-4	69.9 ± 11	1.7 ± 0.3	20.6 ± 2	20.1 ± 4	12
Ex-4+8pCPT	36.4 ± 3*	1.6 ± 0.2	32.6 ± 4*	5.8 ± 1**	14
Change	−47.9%	−5.6%	−58.6%	−70.8%	

Representative data from cells recorded from the same culture on the same day. Each condition was carried out twice with cells of two different cultures, obtaining similar results. Data are expressed as means ± SEM in the units in parentheses. In all cases, *$p < 0.05$ and **$p < 0.01$ (Mann-Whitney U test).

Each cell provides at least 30 spikes, which pass the criteria specified in STAR Methods.

treated with Ex-4, in agreement with the frequency analysis of secretory events obtained with single-cell amperometry experiments (Figure 2C).

CgA release is increased by GLP-1R activation

Results from the amperometry and Cm experiments suggest that the effects of Ex-4 on CA secretion is not from modulation of the number of vesicles undergoing fusion but rather the kinetics of fusion, allowing more CA to escape the vesicle. Chromogranin A (CgA) is a key constituent of secretory granules in chromaffin cells whose secretion may also be modified by GLP-1Rs, especially if the modulation promotes full fusion of vesicles. To test this idea, we developed a protocol to measure CA and CgA secretion in parallel from chromaffin cells. CA secretion was continuously recorded by on-line electrochemical detection and the perfusate collected for dot blotting analysis. Cells were stimulated with repeated 10-s pulses of 10 μM dimethyphenylpiperazinium (DMPP) applied at 5-min intervals. A representative recording is shown in Figure 3A. This is the typical time course of release with this protocol. When Ex-4 and IBMX were added to the perfusion buffer (6th to 10th pulses), the amount of CAs released significantly increased (Figure 3B). Cell perfusion with Ex-4 and IBMX also dramatically increased the amount CgA released (Figure 3D).

Ex-4 increases the release of CgA-EGFP from the chromaffin granules

Since CgA is an 49-kDa protein, an increase in release could results from either an increase in the size or longevity of the fusion pore or an enhancement of disaggregation of the granule matrix. To explore further the effects of GLP-1R activation on exocytosis, we used total internal reflection fluorescence microscopy (TIRFM) to image single vesicle fusion events. Chromaffin cells transfected with CgA-EGFP plasmid (for 24 h) were stimulated with 10 μM DMPP. When granules containing CgA-EGFP fuse with the membrane, the increase in vesicular pH results in an increase in fluorescence intensity that persists while the release of the granule content occurs (Abbineni et al., 2019; Dominguez et al., 2014). For analysis purposes, and to synchronize all measured fusion events, we set the time at the moment of granule fusion at 0 s (Figure 4A). Analysis of all observed exocytotic events showed that almost half of the events presented as partial release, whereas the other half represented full release in control cells (53% of partial release versus 47% of full release; Figure 4D). Partial-release events were those events where the vesicle continues to fluoresce after the fusion (Figure 4B), indicating that the granule released only part of its content. Full-release events were those in which the fluorescence intensity of the granule completely disappeared after fusion with the plasma membrane (Figure 4C). In cells treated with Ex-4, the proportion of full-release events significantly increased to 71% (Figure 4D).

DISCUSSION

The secretory response of adrenal medullary tissues must be tightly controlled, since the large amounts of CA stored within the chromaffin cells that make up the gland would be life threatening if they were all suddenly released (Borges, 1997). The regulation occurs at various levels, from activation of receptors resulting from splanchnic-mediated responses (nicotinic, muscarinic, pituitary adenylate cyclase-activating polypeptide [PACAP], substance P, and vasoactive intestinal peptide [VIP]) (Carbone et al., 2019) to those exerted by hormones, such as histamine, bradykinin, and angiotensin II (Alvarez et al., 1997). Activation of G-protein-coupled receptors on chromaffin cells in turn has been shown to modulate channels, transporters, the calcium signals regulating exocytosis, and priming of releasable vesicles to fine-tune CA output to meet demand under different stress conditions (Aunis, 1998; Carbone et al., 2019). The existence of different degrees of exocytosis, from "kiss-and-run" to full collapsing release, represents another important way to regulate the amount of vesicle cargo liberated from each individual exocytotic event. Comparison of data from patch amperometry (Albillos et al., 1997; Montesinos et al., 2008) and vesicle impact electrochemical cytometry (Dunevall et al., 2017) with conventional amperometry indicates that only 30%–40% of the CA cargoes are normally released on single-event exocytosis (Montesinos et al., 2008). The regulation of this latter process might involve structural mechanisms such the dilation and duration of fusion pore as well as the association of CAs with intravesicular components of the granule matrix (Abbineni et al., 2019; Montesinos et al., 2008; Zhang et al., 2019). The recent description indicating that the amount of CA released can

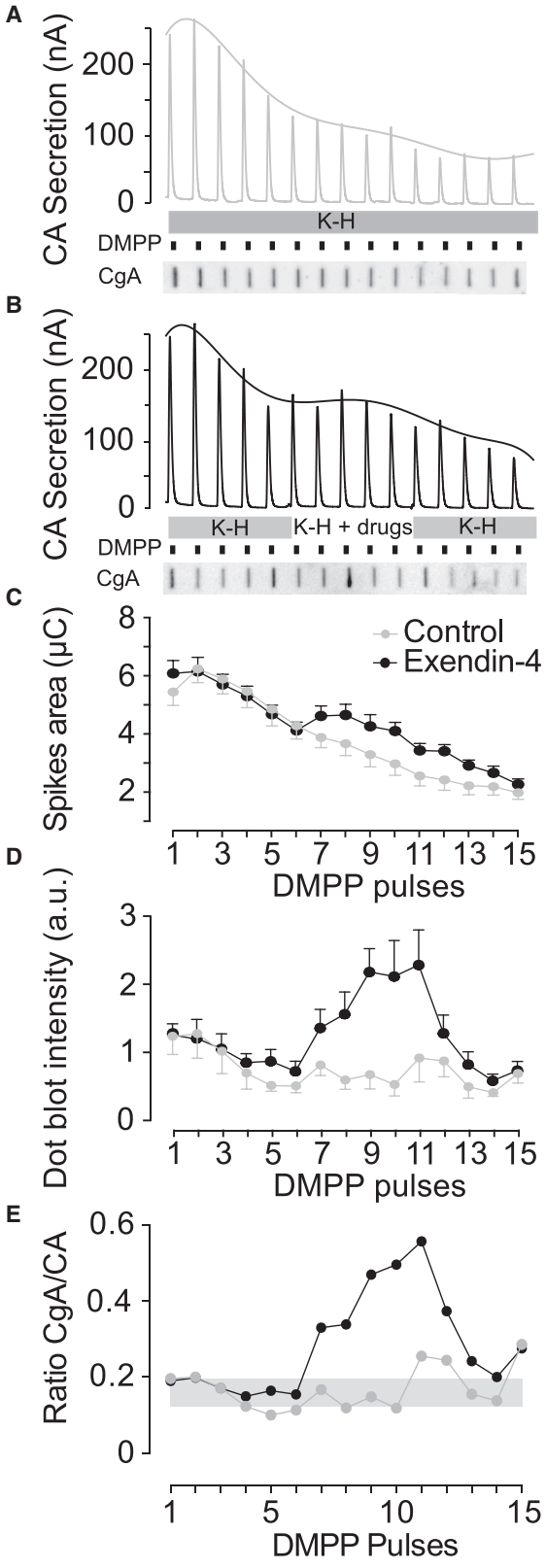

be modified without changing the number of vesicles released probably means that many publications on adrenal regulation just explained on the basis of more or less secretory vesicle (SV) released might need to be revisited.

Here, we have centered our attention on GLP-1R. While the signaling and function of GLP-1Rs has been studied extensively in β cells (Fletcher et al., 2016; Jones et al., 2018; Tomas et al., 2020), knowledge of their extra-pancreatic activity is very limited, despite the wide interest in targeting these receptors for a variety of conditions in addition to type 2 diabetes (Andersen et al., 2018). Although the presence of GLP-1R has been described in PC12 cells (Perry et al., 2002), to the best of our knowledge, all studies published so far were not related to secretion (Qiu et al., 2016; Wang et al., 2018; Zhang et al., 2015; Zhao et al., 2019a), and no studies on chromaffin cells have been reported.

The receptor for GLP-1 is particularly interesting in chromaffin cells, as its main secretory product, adrenaline, is one of the main counteracting anti-insulin hormones. GLP-1R can favor the insulin hypoglycemia and also modulate the effect of insulin by promoting adrenaline release (Verberne et al., 2016) .

The presence of GLP-1R in bovine chromaffin cells was confirmed by a combination of RT-PCR (Figure S1), microscopy (Figure S2), western blot (Figure S3), protein analyses (Figures 1E and F), and functional responses (Figures 2 and 3). Although membrane traffic is out of the scope of this paper, the unusual accumulation of GLP-1R in the cytosol (Figure S2) might reveal an intense up-/downregulation, suggesting that this receptor could be an important actor in the homeostatic control of adrenomedullary response. Although we have not explored the functional significance of this intracellular receptor pool in this paper, the importance of trafficking of GLP-1R on regulating signaling in pancreatic β cells is well recognized (Tomas et al., 2020).

Our functional studies on GLP-1R in chromaffin cells show that its activation does not directly trigger the release of CA but rather enhances their secretory responses to physiological stimuli. Hence, its activation (1) upregulated the expression of TH (Figures 1E and F) through the activation of its gene (Figure 1G), (2) potentiated the synthesis of CAs (Figures 1A–1D), and (3) increased the secretory responses to nicotinic stimuli (Figure 2B). This was caused not by an increase of the releasable pool of the

Figure 3. Ex-4 potentiates the secretion of CgA as well as CAs from chromaffin cells

(A and B) Representative on-line measurements from perfused chromaffin cells. Each current peak indicates CA secretion induced by 12 successive stimuli with 10 µM DMPP in the absence (A) or presence of 100 nM Ex-4 and 500 µM IBMX (B). Below each recording is shown a representative dot blot probed for CgA obtained from the same experiment.

(C) Average peak area (total CA) measured from control cells (n = 14) and cells treated with Ex-4 and IMBX (n = 10). The difference between the 1–5 pulses from control and treated cells shows a p = 0.27, the difference between 5–10 shows a p = 0.04*, and the difference between 10–15 pulses shows a p = 0.09; *p < 0.05, Student's t test.

(D) Average blot intensity obtained from dot-blots from control cells (n = 8) and cells treated with Ex-4 and IMBX (n = 8). The difference between the 1-5 pulses from control and treated cells show a p = 0.87, the difference between 5–10 is p = 0.003** and 10–15 pulses is p = 0.09; **p < 0.01, Student's t test.

(E) Ratios of chromogranin A versus CAs during the perifusion of chromaffin cells with Ex-4. Data obtained from panels C and D. Gray band indicates 95% confidence interval.

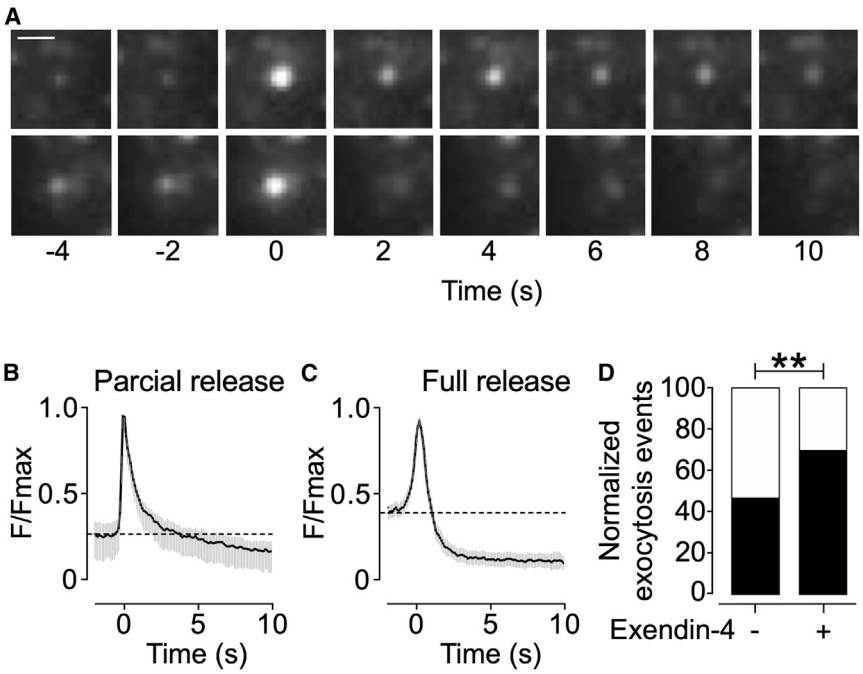

Figure 4. Ex-4 increases the number of full-fusion events

(A) Representative examples of the two modes of CgA-EGFP exocytosis in transfected bovine chromaffin cells, with sequential frames showing partial (top panel) and full release (bottom panel). Scale bar, 1 μm.

(B and C) Average traces of the fluorescent signal from partial-release events (B) and full-release events (C) from cells treated with Ex-4 (incubation time, 20 min).

(D) Normalized distribution of 17 exocytotic events analyzed in 10 control cells and 34 exocytotic events analyzed in 15 cells treated with Ex-4.

**$p < 0.01$, binomial test. Open bar represents partial release, and solid bar represents full release.

vesicles (Figures 2C and S4) but by (4) increasing the amount of cargo released by each quanta (Table 1; Figure S4). Furthermore, we showed that the effects of GLP-1R on CA secretion occurred through the activation of cAMP/PKA, but apparently not through the Epac pathway (Table 2).

The effects of short incubation with Ex-4 on the quantum size and on the kinetics of exocytosis are intriguing, as modulation of CA release at this level has not been reported previously for a G-protein-coupled receptor. On average, CAs are strongly concentrated inside chromaffin granules. Direct measurements estimated adrenaline concentration as large as 0.8–1 M (Albillos et al., 1997; Montesinos et al., 2008). As mentioned above, only a fraction of it seems to be released during "standard" exocytosis that could be addressed to partial exocytosis. Although long-term (24 h) incubation with Ex-4 increased the synthesis and CA cell content, the effect of a short treatment (20 min) on quantum size was due to not an increase in the synthesis but to a large discharge of granule cargo by a shift from a partial- to full-fusion exocytotic mode. These effects contrast with those observed in pancreatic β cells, where the rise in cAMP promotes, through the activation of Epac2, the constriction of the fusion pore and the retention of vesicle cargo (Guček et al., 2019).

CgA is an acidic intragranular protein of ~49 kDa that binds CA with high capacity and low affinity (Helle et al., 2018). In chromaffin cells, we demonstrated a drastic reduction in quantum size when it is absent (Montesinos et al., 2008) and an increase when CgA is overexpressed (Dominguez et al., 2014). This protein and its derived peptides are released along with CA, being the first historical proof that CAs are released by exocytosis (Banks and Helle, 1965). Chromogranins and other intravesicular cargo proteins have been used as tools to estimate the functional diameter of fusion pores based on their molecular weight and hydrated molecular diameters (Steyer and Almers, 2001; Steyer et al., 1997; Zhang et al., 2019). The ratio CgA/CA largely increased when Ex-4 was added to the perifusion buffer, indicating an increase in the number of full fusions (Figure 3D). Also, TIRFM observations revealed that cells switched from partial to full exocytosis upon treatment with Ex-4 (Figure 4).

The main second messenger mobilized by GLP-1R activation is cAMP. We previously described an increase in quantum size caused by cAMP acting through the canonical PKA pathway (Machado et al., 2001). Other agents, such as estrogens or β-sympathetic agents, also promote similar effects on exocytosis (Machado et al., 2001, 2002). However, there are some important differences between those data and the effects of GPL-1R described in the present work. Modest rises in cAMP, like those promoted by estrogens (Machado et al., 2002) or isoproterenol (Machado et al., 2001), slow down the granule emptying kinetics without modifying the apparent quantum size. However, when cAMP levels are strongly elevated or the classical route involving PKA activation is stimulated (e.g., forskolin or okadaic acid), the slow-releasing kinetics are accompanied by a significant increase in quantum size (Machado et al., 2001). The effects of Ex-4 observed in this paper, in spite of being carried out in the same laboratory, showed the acceleration of exocytotic events (larger m and I_{max}), an effect that was potentiated by IBMX and antagonized by H-89 (Tables 1 and 2) (Kobayashi et al., 1999).

We cannot offer an easy explanation to these differences; however, differences in the spatial and temporal properties of cAMP increases induced by different stimulus conditions may impact on downstream effectors, as observed in β cells (Buenaventura et al., 2019; Lester et al., 1997).

Given the fact that GLP-1R agonists are gaining interest as a coadjutant treatment of diabetes, the role of these drugs on the adrenal-sympathetic axis should be taken into account. If our observations extend to the sympathetic system, then we would expect that even though the activation of GLP-1Rs would

not activate it per se, they would potentiate sympathetic responses. In fact, treatment with GLP-1R agonists such as liraglutide or exenatide lower blood pressure (Zhao et al., 2019b), probably by β-receptor activation. However, GLP-1R activation strongly potentiates the responses to stress (Holt and Trapp, 2016), probably through an amphetamine-like effect. Interestingly, increases in neuronal DA have also been reported in several rodent models of Parkinson's disease following treatment with Ex-4 (Athauda and Foltynie, 2018), suggesting that GLP-1R activation of CA may also occur in central TH-positive neurons.

Our working hypothesis explains how stimulation of PKA increases the apparent quantum size by causing a release of a larger fraction of CgA. This effect could result from a longer-lived pore or a larger dissociation of granule matrix.

In this paper, we have described the role of GLP-1R in the regulation of the stimulus-secretion coupling in adrenomedullary tissues. We propose that this target may be involved in the physiological regulation of general homeostasis by the adrenal medulla, which would be physiologically involved in the regulation of general mechanisms such as glycaemia, stress, and blood pressure.

STAR★METHODS

Detailed methods are provided in the online version of this paper and include the following:

- KEY RESOURCES TABLE
- RESOURCE AVAILABILITY
  - Lead contact
  - Materials availability
  - Data and code availability
- EXPERIMENTAL MODEL AND SUBJECT DETAILS
  - Bovine chromaffin cells culture
- METHOD DETAILS
  - On-Line analysis of catecholamine release
  - RNA isolation, cDNA synthesis, and PCR
  - Plasma membrane and cytosol-enriched fractions
  - Immunofluorescence
  - Electrophysiology
  - Measurement of Cytosolic-Free Ca^{2+}
- QUANTIFICATION AND STATISTICAL ANALYSIS

SUPPLEMENTAL INFORMATION

Supplemental information can be found online at https://doi.org/10.1016/j.celrep.2021.109609.

ACKNOWLEDGMENTS

This work was supported by Spanish MINECO (BFU2017-82618-P).

We thank Dr. Alessandro Bisello (Division of Endocrinology and Metabolism, University of Pittsburgh School of Medicine) for providing the human GLP-1R-EGFP plasmid (Syme et al., 2006) and Dr. Esther Louise Sabban (Department of Biochemistry and Molecular Biology, New York Medical College) for supplying the rat TH promoter, p5′TH-Luc (−272/+27) (Nakashima et al., 2003). We also thank to Dr. Pablo Montenegro Escudero for experimental support and personnel of the "Matadero Insular de Tenerife" for providing cow adrenal glands. A.G.-S. had an FPI fellowship from MINECO.

AUTHOR CONTRIBUTIONS

J.D.M.P. conceived the study, designed the experiments, and wrote the paper. A.G.-S. and J.E.-H. performed the experiments. E.P.S. and R.B. analyzed the data and wrote the paper.

DECLARATION OF INTERESTS

The authors declare no competing interests.

Received: July 7, 2020
Revised: July 2, 2021
Accepted: August 4, 2021
Published: August 24, 2021

REFERENCES

Abbineni, P.S., Bittner, M.A., Axelrod, D., and Holz, R.W. (2019). Chromogranin A, the major lumenal protein in chromaffin granules, controls fusion pore expansion. J. Gen. Physiol. *151*, 118–130.

Albillos, A., Dernick, G., Horstmann, H., Almers, W., Alvarez de Toledo, G., and Lindau, M. (1997). The exocytotic event in chromaffin cells revealed by patch amperometry. Nature *389*, 509–512.

Alvarez, C., Lorenzo, C., Santana, F., and Borges, R. (1997). Interaction between G protein-operated receptors eliciting secretion in rat adrenals. A possible role of protein kinase C. Biochem. Pharmacol. *53*, 317–325.

Álvarez de Toledo, G., Montes, M.Á., Montenegro, P., and Borges, R. (2018). Phases of the exocytotic fusion pore. FEBS Lett. *592*, 3532–3541.

Andersen, A., Lund, A., Knop, F.K., and Vilsbøll, T. (2018). Glucagon-like peptide 1 in health and disease. Nat. Rev. Endocrinol. *14*, 390–403.

Athauda, D., and Foltynie, T. (2018). Protective effects of the GLP-1 mimetic exendin-4 in Parkinson's disease. Neuropharmacology *136* (*Pt B*), 260–270.

Aunis, D. (1998). Exocytosis in chromaffin cells of the adrenal medulla. Int. Rev. Cytol. *181*, 213–320.

Baggio, L.L., and Drucker, D.J. (2007). Biology of incretins: GLP-1 and GIP. Gastroenterology *132*, 2131–2157.

Banks, P., and Helle, K. (1965). The release of protein from the stimulated adrenal medulla. Biochem. J. *97*, 40C–41C.

Baraibar, A.M., de Pascual, R., Camacho, M., Domínguez, N., David Machado, J., Gandía, L., and Borges, R. (2018). Distinct patterns of exocytosis elicited by Ca^{2+}, Sr^{2+} and Ba^{2+} in bovine chromaffin cells. Pflugers Arch. *470*, 1459–1471.

Barroso-González, J., Machado, J.D., García-Expósito, L., and Valenzuela-Fernández, A. (2009). Moesin regulates the trafficking of nascent clathrin-coated vesicles. J. Biol. Chem. *284*, 2419–2434.

Bauer, C.S., Woolley, R.J., Teschemacher, A.G., and Seward, E.P. (2007). Potentiation of exocytosis by phospholipase C-coupled G-protein-coupled receptors requires the priming protein Munc13-1. J. Neurosci. *27*, 212–219.

Borges, R. (1997). The rat adrenal gland in the study of the control of catecholamine secretion. Semin. Cell Dev. Biol. *8*, 113–120.

Borges, R., Sala, F., and García, A.G. (1986). Continuous monitoring of catecholamine release from perfused cat adrenals. J. Neurosci. Methods *16*, 289–300.

Buenaventura, T., Bitsi, S., Laughlin, W.E., Burgoyne, T., Lyu, Z., Oqua, A.I., Norman, H., McGlone, E.R., Klymchenko, A.S., Corrêa, I.R., Jr., et al. (2019). Agonist-induced membrane nanodomain clustering drives GLP-1 receptor responses in pancreatic beta cells. PLoS Biol. *17*, e3000097.

Carbone, E., Borges, R., Eiden, L.E., García, A.G., and Hernández-Cruz, A. (2019). Chromaffin cells of the adrenal medulla: Physiology, pharmacology, and disease. Compr. Physiol. *9*, 1443–1502.

Colliver, T.L., Hess, E.J., Pothos, E.N., Sulzer, D., and Ewing, A.G. (2000). Quantitative and statistical analysis of the shape of amperometric spikes recorded from two populations of cells. J. Neurochem. *74*, 1086–1097.

Dickson, P.W., and Briggs, G.D. (2013). Tyrosine Hydroxylase. Adv. Pharmacol. *68*, 13–21.

Domínguez, N., Rodríguez, M., Machado, J.D., and Borges, R. (2012). Preparation and culture of adrenal chromaffin cells. Methods Mol. Biol. *846*, 223–234.

Dominguez, N., Estevez-Herrera, J., Borges, R., and Machado, J.D. (2014). The interaction between chromogranin A and catecholamines governs exocytosis. FASEB J. *28*, 4657–4667.

Doyle, M.E., and Egan, J.M. (2007). Mechanisms of action of glucagon-like peptide 1 in the pancreas. Pharmacol. Ther. *113*, 546–593.

Dunevall, J., Majdi, S., Larsson, A., and Ewing, A. (2017). Vesicle impact electrochemical cytometry compared to amperometric exocytosis measurements. Curr. Opin. Electrochem. *5*, 85–91.

Estévez-Herrera, J., Domínguez, N., Pardo, M.R., González-Santana, A., Westhead, E.W., Borges, R., and Machado, J.D. (2016). ATP: The crucial component of secretory vesicles. Proc. Natl. Acad. Sci. USA *113*, E4098–E4106.

Fader, D., and Lewis, E.J. (1990). Interaction of cyclic AMP and cell-cell contact in the control of tyrosine hydroxylase RNA. Brain Res. Mol. Brain Res. *8*, 25–29.

Fletcher, M.M., Halls, M.L., Christopoulos, A., Sexton, P.M., and Wootten, D. (2016). The complexity of signalling mediated by the glucagon-like peptide-1 receptor. Biochem. Soc. Trans. *44*, 582–588.

Gillis, K.D., Mossner, R., and Neher, E. (1996). Protein kinase C enhances exocytosis from chromaffin cells by increasing the size of the readily releasable pool of secretory granules. Neuron *16*, 1209–1220.

Goldstein, D.S. (2010). Adrenal responses to stress. Cell. Mol. Neurobiol. *30*, 1433–1440.

Guček, A., Gandasi, N.R., Omar-Hmeadi, M., Bakke, M., Døskeland, S.O., Tengholm, A., and Barg, S. (2019). Fusion pore regulation by cAMP/Epac2 controls cargo release during insulin exocytosis. eLife *8*, e41711.

Helle, K.B., Metz-Boutigue, M.H., Cerra, M.C., and Angelone, T. (2018). Chromogranins: from discovery to current times. Pflugers Arch. *470*, 143–154.

Holt, M.K., and Trapp, S. (2016). The physiological role of the brain GLP-1 system in stress. Cogent Biol. *2*, 1229086.

Jahn, R., Lang, T., and Südhof, T.C. (2003). Membrane fusion. Cell *112*, 519–533.

Jones, B., Buenaventura, T., Kanda, N., Chabosseau, P., Owen, B.M., Scott, R., Goldin, R., Angkathunyakul, N., Corrêa, I.R., Jr., Bosco, D., et al. (2018). Targeting GLP-1 receptor trafficking to improve agonist efficacy. Nat. Commun. *9*, 1602.

Kawagoe, K.T., Zimmerman, J.B., and Wightman, R.M. (1993). Principles of voltammetry and microelectrode surface states. J. Neurosci. Methods *48*, 225–240.

Kobayashi, H., Yamamoto, R., Kitamura, K., Niina, H., Masumoto, K., Minami, S.I., Yanagita, T., Izumi, F., Aunis, D., Eto, T., and Wada, A. (1999). Cyclic AMP-dependent synthesis and release of adrenomedullin and proadrenomedullin N-terminal 20 peptide in cultured bovine adrenal chromaffin cells. Eur. J. Biochem. *263*, 702–708.

Lester, L.B., Langeberg, L.K., and Scott, J.D. (1997). Anchoring of protein kinase A facilitates hormone-mediated insulin secretion. Proc. Natl. Acad. Sci. USA *94*, 14942–14947.

Machado, J.D., Segura, F., Brioso, M.A., and Borges, R. (2000). Nitric oxide modulates a late step of exocytosis. J. Biol. Chem. *275*, 20274–20279.

Machado, J.D., Morales, A., Gomez, J.F., and Borges, R. (2001). cAmp modulates exocytotic kinetics and increases quantal size in chromaffin cells. Mol. Pharmacol. *60*, 514–520.

Lindau, M., and Neher, E. (1988). Patch-clamp techniques for time-resolved capacitance measurements in single cells. Pflugers Arch *411*, 137–46.

Machado, J.D., Alonso, C., Morales, A., Gómez, J.F., and Borges, R. (2002). Nongenomic regulation of the kinetics of exocytosis by estrogens. J. Pharmacol. Exp. Ther. *301*, 631–637.

Machado, D.J., Montesinos, M.S., and Borges, R. (2008). Good practices in single-cell amperometry. Methods Mol. Biol. *440*, 297–313.

Mollard, P., Seward, E.P., and Nowycky, M.C. (1995). Activation of nicotinic receptors triggers exocytosis from bovine chromaffin cells in the absence of membrane depolarization. Proc. Natl. Acad. Sci. USA *92*, 3065–3069.

Montesinos, M.S., Machado, J.D., Camacho, M., Diaz, J., Morales, Y.G., Alvarez de la Rosa, D., Carmona, E., Castañeyra, A., Viveros, O.H., O'Connor, D.T., et al. (2008). The crucial role of chromogranins in storage and exocytosis revealed using chromaffin cells from chromogranin A null mouse. J. Neurosci. *28*, 3350–3358.

Moro, M.A., López, M.G., Gandía, L., Michelena, P., and García, A.G. (1990). Separation and culture of living adrenaline- and noradrenaline-containing cells from bovine adrenal medullae. Anal. Biochem. *185*, 243–248.

Müller, T.D., Finan, B., Bloom, S.R., D'Alessio, D., Drucker, D.J., Flatt, P.R., Fritsche, A., Gribble, F., Grill, H.J., Habener, J.F., et al. (2019). Glucagon-like peptide 1 (GLP-1). Mol. Metab. *30*, 72–130.

Nakashima, A., Ota, A., and Sabban, E.L. (2003). Interactions between Egr1 and AP1 factors in regulation of tyrosine hydroxylase transcription. Brain Res. Mol. Brain Res. *112*, 61–69.

Neher, E. (2018). Neurosecretion: what can we learn from chromaffin cells. Pflugers Arch. *470*, 7–11.

Neher, E., and Marty, A. (1982). Discrete changes of cell membrane capacitance observed under conditions of enhanced secretion in bovine adrenal chromaffin cells. Proc. Natl. Acad. Sci. USA *79*, 6712–6716.

Neher, E., and Sakaba, T. (2008). Multiple roles of calcium ions in the regulation of neurotransmitter release. Neuron *59*, 861–872.

Perrais, D., Kleppe, I.C., Taraska, J.W., and Almers, W. (2004). Recapture after exocytosis causes differential retention of protein in granules of bovine chromaffin cells. J. Physiol. *560*, 413–428.

Perry, T., Lahiri, D., Chen, D., Zhou, J., Shaw, K., Egan, J., and Greig, N. (2002). A Novel Neutrotrophic Property Of Glucagon-Like Peptide 1: A Promoter Of Nerve Growth Factor-Mediated Differentiation In PC12 Cells. J. Peripher. Nerv. Syst. *7*, 205–206.

Piech-Dumas, K.M., and Tank, A.W. (1999). CREB mediates the cAMP-responsiveness of the tyrosine hydroxylase gene: use of an antisense RNA strategy to produce CREB-deficient PC12 cell lines. Brain Res. Mol. Brain Res. *70*, 219–230.

Powell, A.D., Teschemacher, A.G., and Seward, E.P. (2000). P2Y purinoceptors inhibit exocytosis in adrenal chromaffin cells via modulation of voltage-operated calcium channels. J. Neurosci. *20*, 606–616.

Qiu, C., Wang, Y.P., Pan, X.D., Liu, X.Y., Chen, Z., and Liu, L.B. (2016). Exendin-4 protects Aβ(1-42) oligomer-induced PC12 cell apoptosis. Am. J. Transl. Res. *8*, 3540–3548.

Segura, F., Brioso, M.A., Gómez, J.F., Machado, J.D., and Borges, R. (2000). Automatic analysis for amperometrical recordings of exocytosis. J. Neurosci. Methods *103*, 151–156.

Shin, W., Ge, L., Arpino, G., Villarreal, S.A., Hamid, E., Liu, H., Zhao, W.D., Wen, P.J., Chiang, H.C., and Wu, L.G. (2018). Visualization of Membrane Pore in Live Cells Reveals a Dynamic-Pore Theory Governing Fusion and Endocytosis. Cell *173*, 934–945.e12.

Sonoda, N., Imamura, T., Yoshizaki, T., Babendure, J.L., Lu, J.-C., and Olefsky, J.M. (2008). Beta-Arrestin-1 mediates glucagon-like peptide-1 signaling to insulin secretion in cultured pancreatic beta cells. Proc. Natl. Acad. Sci. USA *105*, 6614–6619.

Steyer, J.A., and Almers, W. (2001). A real-time view of life within 100 nm of the plasma membrane. Nat. Rev. Mol. Cell Biol. *2*, 268–275.

Steyer, J.A., Horstmann, H., and Almers, W. (1997). Transport, docking and exocytosis of single secretory granules in live chromaffin cells. Nature *388*, 474–478.

Syme, C.A., Zhang, L., and Bisello, A. (2006). Caveolin-1 regulates cellular trafficking and function of the glucagon-like Peptide 1 receptor. Mol. Endocrinol. *20*, 3400–3411.

Taraska, J.W., Perrais, D., Ohara-Imaizumi, M., Nagamatsu, S., and Almers, W. (2003). Secretory granules are recaptured largely intact after stimulated exocytosis in cultured endocrine cells. Proc. Natl. Acad. Sci. USA *100*, 2070–2075.

Thompson, A., and Kanamarlapudi, V. (2015). Agonist-induced internalisation of the glucagon-like peptide-1 receptor is mediated by the Gαq pathway. Biochem. Pharmacol. *93*, 72–84.

Tomas, A., Jones, B., and Leech, C. (2020). New Insights into Beta-Cell GLP-1 Receptor and cAMP Signaling. J. Mol. Biol. *432*, 1347–1366.

Verberne, A.J.M., Korim, W.S., Sabetghadam, A., and Llewellyn-Smith, I.J. (2016). Adrenaline: insights into its metabolic roles in hypoglycaemia and diabetes. Br. J. Pharmacol. *173*, 1425–1437.

Voets, T. (2000). Dissection of three Ca2+-dependent steps leading to secretion in chromaffin cells from mouse adrenal slices. Neuron *28*, 537–545.

Vollmer, R.R., Balcita, J.J., Sved, A.F., and Edwards, D.J. (1997). Adrenal epinephrine and norepinephrine release to hypoglycemia measured by microdialysis in conscious rats. Am. J. Physiol. *273*, R1758–R1763.

Wang, Y., Chen, S., Xu, Z., Chen, S., Yao, W., and Gao, X. (2018). GLP-1 receptor agonists downregulate aberrant GnT-III expression in Alzheimer's disease models through the Akt/GSK-3β/β-catenin signaling. Neuropharmacology *131*, 190–199.

Wightman, R.M., Jankowski, J.A., Kennedy, R.T., Kawagoe, K.T., Schroeder, T.J., Leszczyszyn, D.J., Near, J.A., Diliberto, E.J., Jr., and Viveros, O.H. (1991). Temporally resolved catecholamine spikes correspond to single vesicle release from individual chromaffin cells. Proc. Natl. Acad. Sci. USA *88*, 10754–10758.

Yim, Y.Y., Zurawski, Z., and Hamm, H. (2018). GPCR regulation of secretion. Pharmacol. Ther. *192*, 124–140.

Zhang, J., Wu, J., Zeng, W., Zhao, Y., and Zu, H. (2015). Exendin-4, a glucagon-like peptide-1 receptor agonist, inhibits Aβ25-35-induced apoptosis in PC12 cells by suppressing the expression of endoplasmic reticulum stress-related proteins. Int. J. Clin. Exp. Pathol. *8*, 12784–12792.

Zhang, Q., Liu, B., Wu, Q., Liu, B., Li, Y., Sun, S., Wang, Y., Wu, X., Chai, Z., Jiang, X., et al. (2019). Differential Co-release of Two Neurotransmitters from a Vesicle Fusion Pore in Mammalian Adrenal Chromaffin Cells. Neuron *102*, 173–183.e4.

Zhao, F., Li, J., Wang, R., Xu, H., Ma, K., Kong, X., Sun, Z., Niu, X., Jiang, J., Liu, B., et al. (2019a). Exendin-4 promotes actin cytoskeleton rearrangement and protects cells from Nogo-A-Δ20 mediated spreading inhibition and growth cone collapse by down-regulating RhoA expression and activation via the PI3K pathway. Biomed. Pharmacother. *109*, 135–143.

Zhao, X., Huang, K., Zheng, M., and Duan, J. (2019b). Effect of liraglutide on blood pressure: a meta-analysis of liraglutide randomized controlled trials. BMC Endocr. Disord. *19*, 4.

Zhou, J., Wang, X., Pineyro, M.A., and Egan, J.M. (1999). Glucagon-like peptide 1 and exendin-4 convert pancreatic AR42J cells into glucagon- and insulin-producing cells. Diabetes *48*, 2358–2366.

STAR★METHODS

KEY RESOURCES TABLE

REAGENT or RESOURCE	SOURCE	IDENTIFIER
Antibodies		
Rabbit polyAb anti-GLP-1R	Abcam	Cat# ab39072, RRID: AB_880213
Monoclonal anti-actin	Sigma-Aldrich	Cat# A3853, RRID: AB_262137
Monoclonal anti-tyrosine hydroxylase	Sigma-Aldrich	Cat# T1299, RRID: AB_477560
Goat polyclonal anti-CgA	Santa Cruz Biotechnology	Cat# sc-1488, RRID: AB_2276319
Secondary horseradish peroxidase-conjugated anti-rabbit IgG	GE Healthcare	Cat# NA934, RRID: AB_772206
Secondary horseradish peroxidase-conjugated anti-mouse IgG	GE Healthcare	Cat# NA931, RRID: AB_772210
Alexa 488-conjugated anti-rabbit	Thermo Fisher Scientific	Cat# A-21206, RRID: AB_2535792
Alexa 568-conjugated anti-mouse	Thermo Fisher Scientific	Cat# A-21124, RRID: AB_2535766
Chemicals, peptides, and recombinant proteins		
Fetal bovine serum	Biowest SAS	Cat# S1810
Horse serum	Biowest SAS	Cat# S0900
Bicinchoninic acid	Sigma-Aldrich	Cat# BCA1
Bovine serum albumin	Sigma-Aldrich	Cat# A8551
Collagenase type IA	Sigma-Aldrich	Cat# C2674
DMEM high glucose	Sigma-Aldrich	Cat# D5648
Glycine	Sigma-Aldrich	Cat# G8898
HEPES	Sigma-Aldrich	Cat# H3375
Oligo(dT)$_{23}$	Sigma-Aldrich	Cat# Q4387
Paraformaldehyde	Sigma-Aldrich	Cat# P6148
Penicillin G	Sigma-Aldrich	Cat# P3032
Percoll	Sigma-Aldrich	Cat# P4937
poly-D-lysine	Sigma-Aldrich	Cat# P1024
RPMI-1640	Sigma-Aldrich	Cat# R6504
Trypan blue	Sigma-Aldrich	Cat# T6146
Tween 20	Sigma-Aldrich	Cat# P2287
Gentamicin	Acofarma	Cat# 1405-41-0
Urografin 76%	Schering España	Cat# 909846.9
Moloney murine Leukemia virus transcriptase	Promega	Cat# M368C
RQ1 RNase-free DNase	Promega	Cat# M610A
Tri-Reagent	Zymo Research	Cat# R2050
Green Taq DNA Polymerase	GenScript	Cat# E00043
Exendin-4	Tocris Bioscience	Cat# 1933
8-pCPT-2-O-Me-cAMP-AM	Tocris Bioscience	Cat# 4853
cOmplete, EDTA-free Protease Inhibitor Cocktail	Roche	Cat# 04693132001
Critical commercial assays		
Steady Glo luciferase system kit	Promega	Cat# E2510
Direct-zol™ RNA miniprep kit	Zymo Research	Cat# R2052
Deposited data		
Raw and analyzed data	This paper	N/A

(*Continued on next page*)

Continued		
REAGENT or RESOURCE	SOURCE	IDENTIFIER
Experimental models: Cell lines		
PC12	ATCC®	CRL-1721
Oligonucleotides		
GLP-1R forward5′-TCCTTCATCC TCCGAGCACT-3′	(IDT) Integrated DNA Technologies	N/A
GLP-1R reverse5′-TGCATGAGCA GGAACACCAG-3′	(IDT) Integrated DNA Technologies	N/A
HPRT *(hypoxanthine phosphoribosyl transferase)* forward5′- CTCATGGAC TGATTATGGACA-3′	(IDT) Integrated DNA Technologies	N/A
HPRT *(hypoxanthine phosphoribosyl transferase)* reverse5′- GCAGGTCA GCAAAGAACTTAT-3′	(IDT) Integrated DNA Technologies	N/A
Recombinant DNA		
Human GLP1-R-EGFP	Syme et al., 2006	N/A
Rat TH promoter p5′TH-Luc (−272/+27	Nakashima et al., 2003	N/A
Mouse CgA-EGFP	Dominguez et al., 2014	N/A
pEGFP-N1 *discontinued* (actually pAcGFP1-N1 Vector)	Clontech-Takara	632469
Software and algorithms		
IGOR-Pro	Wavemetrics	https://www.wavemetrics.com
Spikes 50 - Macros for Igor-Pro that allows Automatic analysis of amperometrical recordings.	Segura et al., 2000	http://rborges.webs.ull.es/protocols-and-software/
Metamorph software	Molecular Devices	https://www.moleculardevices.com/products/cellular-imaging-systems/acquisition-and-analysis-software/metamorph-microscopy#gref
Prism® Software	Graphpad	https://www.graphpad.com/scientific-software/prism/

RESOURCE AVAILABILITY

Lead contact

Further information and requests for resources and reagents should be directed to and will be fulfilled by the lead contact, José David Machado Ponce (david.machado@ull.edu.es).

Materials availability

This study did not generate new unique reagents.

Data and code availability

- This study did not generate/analyze datasets/code.
- Any information required to reanalyze the data reported in this paper is available from the lead contact upon request.

EXPERIMENTAL MODEL AND SUBJECT DETAILS

Bovine chromaffin cells culture

Cells were isolated by adrenal medulla digestion as described by (Domínguez et al., 2012; Moro et al., 1990). Briefly, adrenal glands were washed with 3-4 mL of warm Locke's solution (150 mM NaCl, 5.6 mM KCl, 3.6 mM $NaHCO_3$, 11 mM glucose, and 10 mM HEPES buffer at pH 7.3). Medulla digestion was carried out by injecting the gland with 3-4 mL of a solution containing 1.5-2 mg/ml of collagenase IA and 3-4 mg/mL of BSA in Locke's solution, followed by 20 min incubation at 37°C. The digestion procedure is repeated three times. Using sterile scalpel and scissors, the gland was opened longitudinally and the digested medulla was separated from the

cortex and transferred to a clean tube. Additional 10 min incubation with collagenase solution was carried out to dissociate the adrenal medullary cells. Cells were filtered first with a sterile cotton gauze and then with a 200-μm nylon mesh. Resuspension in fresh Locke's solution and centrifugation at 900 x g for 5 min were followed after each filtration step. In order to purify the chromaffin cells, the cells obtained in the previous step were resuspended in fresh Locke's solution and mixed with 15% Urografin solution to obtain a final Urografin concentration of 7.5%. The new cell suspension with 7.5% Urografin was carefully added onto the surface of 15% Urografin solution in centrifuge tubes. The chromaffin cells appeared as a diffuse band at the interface of the two Urografin solutions after centrifugation at 7500 x g for 20 min at 18°C. Chromaffin cells were washed twice in Locke's solution and resuspended in (1:1) DMEM and Ham's-F12 medium supplemented with 10% fetal bovine serum, 50 IU mL^{-1} penicillin and 50 mg · mL^{-1} gentamicin. Finally, the cells were filtered with a 90-μm nylon mesh, counted using trypan blue and plated on Petri dishes, plates or coverslips, depending on the experimental procedure. The cells were maintained in an incubator at 37°C in a humidified chamber at 5% CO_2 and the medium changed by replacing 50% with fresh medium every 2 days.

PC12 cells (ATCC® CRL-1721) were grown in RPMI-1640 media supplemented with 5% fetal bovine serum and 5% horse serum, as well as the aforementioned antibiotics. The cells were maintained at 37°C in a humidified atmosphere with 5% CO_2 and passaged regularly every 2–3 days. In order to preserve their neural phenotype, only non-attached cells were passaged and used.

METHOD DETAILS

Cell transfection. PC12 cells ($3 \cdot 10^6$ cells per cuvette) were transfected using a Nucleofector II device (Lonza, Verviers, Belgium) and the protocol (U-029) with DNA construct. A specific Amaxa-kit was used for delivery 2 μg of cDNA. The experiments were performed between 24 – 48 h after transfection.

Chemiluminescence. Firefly luciferase activity was determined using Steady Glo Luciferase System (Promega) according to the manufacturer's instructions. PC12 cells were lysed with 50 μL of the luciferase substrate and 50 μL of PBS. The luminescence was measured immediately with a Victor X Luminescence Plate Reader (Perkin-Elmer). Luciferase activity was normalized to protein concentration of the samples determined using bicinchoninic method. At least four cell culture plates were used for each treatment. All experiments were performed twice.

Western blotting. The extent of protein expression was assessed by western blot of cell lysates. Cells were lysed at different time points for 20 min at 4°C in lysis solution TENT (mM): Tris HCl (50), EDTA (5), NaCl (150) and 1% Triton X-100, with the protease inhibitor mixture cOmplete® (11697498001 Roche Diagnostics, Mannheim, Germany). Equivalent amounts of proteins were separated by SDS–PAGE using 10% acrylamide gels and electroblotted onto 0.45 μm polyvinylidene difluoride membranes (Immobilon-P IPVH00010 Millipore Corporation, Billerica, MA, USA). Cell lysates were immunoblotted with specific antibodies. To confirm the selectivity of the GLP-1R antibody, we tested the lack of labeling in non-ectodermic cells using HEK293 as negative control versus bovine chromaffin and PC12 cells, showing no labeling in the former. Also, the antibody labels the membrane fraction of PC12 cells. Protein bands were detected by luminescence using an ECL-prime Western Blotting Detection Reagent (RPN2232 GE, Health Care, UK), and protein bands were analyzed using a ChemiDoc MP VersaDoc device and Quantity One 4.6.7 software (Bio-Rad, Hercules, CA, USA).

HPLC analysis of catecholamines. Chromaffin cells and PC12 ($1 \cdot 10^6$) cells were triturated in ice-cold lysis buffer containing perchloric acid (0.05 N) and 3,4-dihydroxybenzylamine (200 nM) as an internal standard. The homogenates were centrifuged and the cleared supernatants were analyzed by HPLC (Shimadzu, Japan) coupled to an electrochemical detector LCB-4 (BioAnalytical Sciences, Bloomington, IN, USA) as described elsewhere (Borges et al., 1986).

Amperometric detection of exocytosis. Chromaffin cells transfected with GLP-1R-EGFP and un-transfected control cells were viewed by epi-fluorescence under an inverted microscope (Olympus IX51, using a 40X/0.60 NA objective). Excitation light (mercury lamp, X-cite EXFO series, 120W) was band-pass–filtered (BP480/20) and the emitted light passed through a dichroic mirror 500 and emission filter (BP520IF; all filters were from Olympus) and imaged with a CCD camera (Orca C4742-80-12AG; Hamamatsu Photonics, Hamamatsu City, Japan). Carbon fiber microelectrodes of 6 μm radius, (Thornel P-55; Amoco Corp., Greenville SC, USA) were prepared as described (Kawagoe et al., 1993) and calibrated to assure the reproducibility of results (Machado et al., 2008). Electrochemical recordings were performed using a VA-10X potentiostat (NPI Electronics, Tamm, Germany) connected to a data acquisition system (PowerLab 8/30, ADInstruments). All amperometric measurements were acquired at 4 kHz and low-pass filtered at 1 kHz. After gently touching the surface of a cell with the carbon fiber microelectrode, secretion was elicited with 5 s pressure ejections of 5 mM $BaCl_2$ (Baraibar et al., 2018). Cells were maintained in Krebs-HEPES buffer solution (K-H), at 37°C for the duration of the recordings.

On-Line analysis of catecholamine release

This method has been described by (Estévez-Herrera et al., 2016). Briefly, chromaffin cells ($4 \cdot 10^6$ cells) plated in plastic Petri dishes (92-mm diameter, Nunc) were cultured for 24-72 h in standard conditions. The cells were then gently removed from the bottom of the dish with a cell scraper, centrifuged at 365xg during 5 min, and re-suspended in 1 mL of K-H buffer. Then, cells were packaged into a 0.22 μm filter that was used as cell chamber (Whatman, GE, Healthcare). The cells were perifused at 37°C with K-H solution at a rate of 2 $mL \cdot min^{-1}$ and the liquid which emanated was conducted to an electrochemical detector with a fixed potential of +650 mV (LC-4B, BioAnalytical Systems), connected to data acquisition hardware PowerLab 8/30 (ADInstruments Ltd, Oxford, UK). Secretion was stimulated every 5 min with 10 s pulses of K-H solution supplemented with DMPP (10 μM). Secretion was quantified by integration

of the amperometric signal. The emanating buffer was also collected in Eppendorf microtubes and stored at −20°C until analysis by dot-blot, being recommended this technical approach for the concentration of secreted proteins and their quantitative determination.

TIRF Microscopy. Chromaffin cells (10^5 cells) plated on coverslip (18-mm diameter, WPI) were visualized on an inverted microscope (200M; Zeiss, Jena, Germany) through a 1.45 NA objective (α Fluar, x100/1.45; Zeiss), as described elsewhere (Barroso-González et al., 2009; Dominguez et al., 2014). Briefly, the objective was coupled to the coverslip with an immersion fluid (n_{488} = 1.518; Zeiss) and for evanescent field illumination, the expanded beam (488 nm) from an argon ion laser (Lasos; Lasertechnik GmbH, Jena, Germany) was band-pass filtered (488/10; Zeiss) and used to excite EGFP. The laser beam was incident to the coverslip at 64-66° from normal; images were captured with EM-CCD digital camera (C9100-13; Hamamatsu Photonics,). Each cell was imaged for up to 1 min with HC Image acquisition software (Hamamatsu Photonics) with a 10 ms exposure time at 10 Hz.

RNA isolation, cDNA synthesis, and PCR

RNA was isolated from purified bovine chromaffin cells using Tri-Reagent (R2050, Sigma) and Direct-zol RNA Miniprep kit (R2052, Zymo Research). Primary chromaffin cell purity reaches 95% using Urografin gradient purification. 4·106 cultured cells were lysated in 800 μL of Tri-Reagent. After adding 200 μL of chloroform and mixing, samples were centrifugated at 12,000 x g for 15 min at 4°C. One volume of absolute ethanol was added to the supernatant, mixed, and then RNA was cleaned and eluted using the Direct-zol RNA miniprep kit, according to the manufacturer's instructions. Genomic DNA contamination was removed adding DNase I (M610A, Promega). The effectiveness of the DNase treatment was assessed in samples with no reverse transcriptase added (RT-negative). Integrity of RNA was checked by agarose gel electrophoresis and finally, the concentration of RNA was determined spectrophotometrically using a NanoDrop ND-1000 (Thermo Scientific).

Retro-transcription was carried out using 2 μL of RNA, and first-strand complementary DNA was synthesized using Moloney murine leukemia virus reverse transcriptase (M368C, Promega) and a 1:1 mix of oligo(dT)23 (Q4387, Sigma-Aldrich) and random hexamers (11-034-731-001, Roche) according to the manufacturer's instructions.

The PCR were carried out for 40 cycles using following sets of primers: 94°, 2 min; 40x (94°, 15 s; 60°, 20 s; 72°, 30 s); 72°, 5 min

forward 5′-TCCTTCATCCTCCGAGCACT-3′
reverse 5′-TGCATGAGCAGGAACACCAG-3′ which amplifies 146 bp of GLP-1R; forward 5′- CTCATGGACTGATTATGGACA-3′
reverse 5′- GCAGGTCAGCAAAGAACTTAT-3′, which amplifies 195 bp of HPRT (hypoxanthine phosphoribosyl transferase).

All PCR experiments were performed using GenScript kit according to the manufacturer's instructions (Promega).

Plasma membrane and cytosol-enriched fractions

PC12 cells were homogenized in 0.25 M sucrose, 1 mM EDTA, 20 mM HEPES, pH 7.4, with protease inhibitor cOmplete®. The lysates were then cleared of unbroken cells by centrifugation (700 × g for 10 min) and subjected to differential centrifugation at 20,000 × g for 20 min. We first isolated plasma membranes by Percoll gradient fractionation. The postnuclear supernatant was layered onto 30% Percoll and sedimented at 84,000 × g for 30 min. The plasma membrane and cytosol fraction were analyzed by western blot.

Immunofluorescence

Chromaffin cells were seeded on 12 mm diameter glass coverslips. After 24 h cells were fixed for 10 min at room temperature (RT) in 2% paraformaldehyde in PBS/150 mM sucrose, then washed three times with PBS and permeabilized with 0.2% Tween-20 in PBS (where indicated). Cell autofluorescence was quenched with 100 mM glycine in PBS. Non-specific binding was reduced by blocking with 5% of BSA in permeabilization solution (or in PBS/150 mM sucrose for non-permeabilized cells) for 1 h at RT. The cells were washed with PBS and immunostained overnight at RT with indicated primary antibodies diluted in PBS/150 mM sucrose. The fluorophore-conjugated secondary antibody was also diluted in PBS/150 mM sucrose for 1 h at RT. Finally, after several washing steps with PBS at RT, coverslips were mounted in Mowiol-antifade (Dako, Glostrup, Denmark) and imaged at high resolution in x-y mid-sections on a Leica confocal microscope TCS SP8 (Leica Microsystems, Wetzlar, Germany). The final images were analyzed with Metamorph software (Universal Imaging Corp., Downington, PA, USA).

Electrophysiology

A coverslip carrying chromaffin cells was placed in a cell chamber on the stage of an inverted phase-contrast Axiovert microscope (Zeiss, Jena, Germany). Cells were perfused with an extracellular solution consisting of 140 mM NaCl, 5 mM NaHCO3, 2 mM KCl, 1 mM MgCl2, 10 mM Glucose, 10 mM HEPES, 2.5 mM CaCl2; pH adjusted to 7.3 with NaOH, 300-310 mOsM. Capacitance measurements were recorded in whole cell-patch-clamp configuration using borosilicate glass electrodes coated with Sylgard 184 (Dow Corning, Midland, MI, USA) and fire-polished to a resistance of 4-6 MΩ. Electrodes were filled with a solution consisting of 145 mM Cs-glutamate (Calbiochem, Nottingham, UK), 10 mM HEPES, 9.5 mM NaCl, 0.3 mM BAPTA (Molecular Probes, Eugene, OR, USA) and 2 mM ATP-Mg; pH adjusted to 7.3 with CsOH (ICN Biomedicals, Aurora, OH, USA). Series resistance was ˂20 MΩ and compensated electronically using a patch-clamp amplifier (HEKA EPC-10; HEKA, Lambrecht, Germany). Capacitance measurements were performed according to the Lindau-Neher technique (Lindau and Neher, 1988) using the 'sine + dc' mode in the Lock-in Extension of

Patchmaster (HEKA). The frequency and peak-to-peak amplitude of the sine wave were 1042 Hz and 30 mV, respectively, and the holding potential was −70 mV. Recordings were sampled at 12.5 kHz and filtered at 2.9 kHz. Ca^{2+} influx was quantified by integrating ICa, omitting the first 2 ms, which were contaminated by Na^{+} currents. Exocytosis was elicited by stimulating cells with a train of 6 X 10 ms step depolarizations to +10 mV followed by 4 X 100 ms step depolarizations to +10 mV (Voets, 2000). Recordings of control cells and cells pretreated for 20 min with 100 nM Ex-4 were alternated and analysis was restricted to the capacitance changes induced by the first stimulus applied after establishing the whole cell recording. Depolarization evoked changes in membrane capacitance (delta Cm) were quantified by averaging 5 points before each step (pre), 5 points 400 ms after the step (post), and then subtracting the former from the latter (ie. post-pre = delta Cm). All experiments were performed at room temperature (21-25°C).

Measurement of Cytosolic-Free Ca^{2+}

This protocol is similar than has been described by Estévez-Herrera et al., 2016. Chromaffin cells were seeded on 12-mm Ø coverslips in 24-well culture plates at a density of ~100,000 cells per well. After 24 h the cells were incubated for 45 min at 37°C with 2 μM Oregon green (Molecular Probes, Invitrogen) in Krebs-HEPES. The cells were then washed for 45 min at room temperature and placed in a chamber mounted on the stage of a Zeiss Axiovert 200 microscope with continuous perfusion. Cells were stimulated with 5 s pulses of DMPP every 4 min. Ex-4 was perifused from 4 min prior to the second pulse and remained bathing cells along the rest of the experiment. Single-cell fluorescence was excited at 488 nm using an argon ion laser (100 ms of excitation every 1 s, 10-nm bandwidth; Lasos, Lasertechnik) and with a EC Plan-Neofluar 20 × /0.50 objective (Zeiss). All measurements were taken at room temperature. Images were collected using a 510-DCLP dichroic mirror and aD525/50 emission filter (Chroma Technology), and then recorded on a CCD camera (AxioCam MRm, Zeiss). Single-cell fluorescence records were plotted against time using the Metamorph software (Universal Imaging).

QUANTIFICATION AND STATISTICAL ANALYSIS

Amperometric data analysis. Data analysis was carried out using IGOR-Pro (Wavemetrics, Lake Oswego, OR, USA). Tailored macros and routines were written to extract the following parameters from each spike: I_{max}, maximum oxidation current, expressed in pA; $t_{1/2}$, spike width at half height, expressed in ms; Q, spike net charge, expressed in pC; m, ascending slope of spike, expressed in pA/ms (Machado et al., 2000; Segura et al., 2000). The foot duration was calculated as the time between the beginning of the spike and the intersection point of the initial slope and the basal line.

The data was analyzed by a second investigator who was blinded to the experimental conditions. To reduce bias caused by the decaying sensitivity of an electrode over time, recordings were alternated between control and test cells; no comparisons were made between experiments carried out on different days. The kinetic parameters were calculated as mean values. The discrimination threshold was fixed at 2.5 SD of the basal noise of the first derivative of each recording. Spikes with an I_{max} over 2.5 pA are usually included in the data analysis. The kinetic parameters were calculated as mean values from at least 20 spikes per cell.

To avoid the deviations caused by the different number of spikes produced by each cell, the average values of spikes parameters recorded from each cell were considered as N = 1 (Colliver et al., 2000). "n, the number of amperometry spikes that were used in the statistical analysis. All of those spikes had to satisfy the following selection criteria:

i. Spikes Imax must be above the detection threshold.
ii. Spikes must not show overlapping.
iii. None of the measured parameters were not affected by any artifact.

Quantitative data may differ from day to day and require daily controls experiments. This is especially important when using transfected cells, since permeabilized procedures greatly affect the secretory machinery. Cumulative secretion was calculated by integration the amperometric signal measured for 2 min and expressed as pico-Coulombs (pC). The results were normalized with respect to the mean their own control.

Image analysis TIRFM. Fluorescence intensity over time was calculated using custom designed routines in Metamorph (Molecular Devices, Sunnyvale, CA, USA) as described previously (Dominguez et al., 2014; Taraska et al., 2003). Briefly, exocytotic events were located by eye, a region of interest (9 pixels- diameter) was centered on the position of the event, and a stack of images in that region was extracted from the movie. The fluorescence intensity profiles from individual granule stacks were plotted against time. In order to differentiate whether a decrease in the fluorescence signal of vesicle was caused by partial exocytosis or from a variation in TIRF plane, we measured the σ changes of the Gaussian function of the fluorescent spots (Dominguez et al., 2014; Perrais et al., 2004; Steyer and Almers, 2001; Taraska et al., 2003) as this parameter increases at the moment of the spread of protein in the media. All exocytotic events were aligned to the frame just before exocytosis.

Statistics. Datasets are expressed as means ± SEM. The statistical significance between groups of experiments was performed by the non-parametric Mann-Whitney rank sum, ANOVA; Dunnett's multiple comparisons test or by Student's t test, where appropriate, based on the D'Agostino-Pearson normality test. The differences were considered significant at the level of $p < 0.05$; data were analyzed using Prism® Software (Graphpad Software, San Diego, USA). No sample calculation was performed. Outliers were not removed from any of the analysis.